Journal of Luminescence 129 (2009) 686–690

Contents lists available at ScienceDirect

Journal of Luminescence

journal homepage: www.elsevier.com/locate/jlumin

Disorder-dependent photoluminescence in $Ba_{0.8}Ca_{0.2}TiO_3$ at room temperature

F.V. Motta [a,*], A.T. de Figueiredo [a], V.M. Longo [a], V.R. Mastelaro [b], A.Z. Freitas [c], L. Gomes [c], N.D. Vieira Jr.[c], E. Longo [a], J.A. Varela [a]

[a] Instituto de Química, UNESP, 14801-970 Araraquara-SP, Brazil
[b] Instituto de Física de São Carlos, USP, 13560-970 São Carlos, SP, Brazil
[c] Center for Lasers and Applications, IPEN, 05508-000 São Paulo, SP, Brazil

ARTICLE INFO

Article history:
Received 30 April 2008
Received in revised form
16 January 2009
Accepted 27 January 2009
Available online 6 February 2009

PACS:
77.84.D
61.43.D
78.60
81.30.H

Keywords:
Titanates
Amorphous semiconductors
Photoluminescence
Order–disorder
BCT

ABSTRACT

The photoluminescence (PL) emission in structurally disordered $Ba_{0.8}Ca_{0.2}TiO_3$ (BCT20) powders was observed at room temperature with laser excitation at lines 355 and 460 nm. The structural evolution perovskite-like titanate BCT20 powders prepared by a soft chemical processing at different annealing temperatures were accompanied by X-ray diffraction (XRD) and X-ray absorption near-edge structure (XANES). Intermediate oxycarbonate phase was identified and your influence with PL emission was discarding. BCT20 annealed at 500 °C displays intense PL emission. The results indicate relationship between broad PL band and order–disorder degree.

1. Introduction

Barium titanate ($BaTiO_3$) single and polycrystalline crystals exhibit phase transformation above room temperature. Cubic $BaTiO_3$ has an ideal perovskite-type structure. The cubic phase transforms into a high temperature hexagonal structure at around 1432 °C. A cubic-to-tetragonal phase transition occurs below 132 °C [1]. Tetragonal $BaTiO_3$ is one of the most extensively investigated photorefractive materials because of its high electro-optic coefficient [1–3].

Barium calcium titanate of the congruently melting composition $Ba_{0.77}Ca_{0.23}TiO_3$ (BCT) is an important electro-optic material for different photorefractive and holographic applications [4–11]. Calcium acts as a reduction inhibitor in $BaTiO_3$, reducing the possibility of the hexagonal phase transition occurring [2]. Jastrabik et al. [12] reported on the optical absorption and luminescence spectra of pure $Ba_{0.77}Ca_{0.23}TiO_3$ and Cr-doped single crystals, which were examined in the spectral range of 300–800 nm and in the temperature range of 5–300 K.

An important discussion concerning the synthesis of BCT is the formation of an intermediate phase. Different authors have concluded that, prior to the formation of $BaTiO_3$, an intermediate can be formed with the overall $Ba_2Ti_2O_5 \cdot CO_3$ composition [13,14].

Disorder in materials can be manifested in many ways: some examples are vibrational, spin and orientation disorder (all corresponding to a periodic lattice) and topological disorder. We will concentrate principally on the latter, which is the type of disorder associated with the structure of glassy and amorphous solids, a structure that cannot be defined in terms of a periodic lattice. Photoluminescence (PL) is a powerful probe of certain aspects of short-range order in the range of 2–5 Å and medium range of 5–20 Å, such as clusters, where the degree of local order is such that structurally inequitable sites can be distinguished because of their different types of electronic transitions and are linked to a specific structural arrangement.

It has been demonstrated that a series of structurally disordered titanates ($ATiO_3$, where A = Ca, Sr and Pb), synthesized by a soft chemical process called the (PPM), have shown intense

* Corresponding author.
E-mail address: fabiana@liec.ufscar.br (F.V. Motta).

0022-2313/$ - see front matter © 2009 Elsevier B.V. All rights reserved.
doi:10.1016/j.jlumin.2009.01.014

PL effect at room temperature when excited by a 488.0 and 350.7 nm laser excitation line [15–18]. X-ray absorption near-edge structure (XANES) results on the $CaTiO_3$ (CT) disordered powders [18,19] pointed to the coexistence of two types of environments for titanium atoms, namely fivefold [TiO_5] square-base pyramid and sixfold coordination [TiO_6] octahedron. The order was related to the presence of [TiO_6] clusters, whereas the disorder was related to the presence of [TiO_5] clusters. This PL emission was attributed to localized levels above the valence band (VB) and below the conduction band (CB).

In addition, theoretical calculus illustrates the electron density maps of $BaTiO_3$ [16]. A homogeneous distribution of the electronic density representing the covalent bonding character of Ti–O and the strongly ionic nature of Ba and O atom bonding has been shown. The formal charge of the symmetric [TiO_6]–[TiO_6] clusters in the ordered structure possesses the same values; hence, the difference of the charge densities is zero. A structural asymmetry occurs in the disordered structure, [TiO_5]–[TiO_6], so the difference between the formal charge of the clusters is $0.5q$ (q = electronic oxygen charge), suggesting the presence of polarization in this system. The charge gradient and the presence of localized states provide a good condition for the trapping of electrons (e') and holes ($h^{\bullet}$) during the excitation process. The recombination $e'/h^{\bullet}$ generates polarons, favoring photoluminescent emission at room temperature in the visible region by disordered $BaTiO_3$ powders. The disordered structure presents a structural asymmetry that leads to differences of formal charge between clusters, suggesting polarization of the system. Moreover, a charge transfer occurs from the [TiO_6] cluster to the [TiO_5] one [16,20].

The aim of this work is to study the properties of PL of $Ba_{0.8}Ca_{0.2}TiO_3$ powder samples and its dependence on the structural order–disorder of the lattice. The PL property of these powders excited by UV and blue light was therefore considered.

2. Experimental procedures

Ordered and disordered BCT20 powders were synthesized by the polymeric precursor method [21,22]. The dark-brown powder obtained was crystallized at several temperatures ranging from 400 to 600 °C for 2 hours using a heating rate of 5 °C/min.

The BCT20 powders were structurally characterized using X-ray diffraction (XRD) (Cu K_α radiation). The diffraction patterns were recorded in a Bragg–Brentano diffractometer (Rigaku 2000) at Cu K_α in a θ–2θ configuration, using a graphite monochromator. Titanium K-edge X-ray absorption near-edge structure spectra were collected at the D04B-XAFS1 beamline at the LNLS-National Laboratory of Synchrotron Light, Campinas, Brazil, storage ring operating at 1.36 GeV and around 160 mA. XANES spectra were collected at the Ti K-edge (4966 eV) in a transmission mode using a Si (111) channel-cut monochromator. To provide good energy reproducibility during the XANES data collection, the energy calibration of the monochromator was checked during the collection of the sample data using a Ti metal foil. For comparison, all the spectra were background removed and normalized using as unity the first extended X-ray absorption fine structure oscillation. The PL spectra were collected with a digital monochromator internally integrated to a CCD with optical resolution of 1 nm and accuracy of 0.1 nm (Newport, OSM-400UV/VIS-U), using a time integration of 4 s (2.9×10^{-17} W/counts s^{-1}) coupled to an optical fiber. The 355 nm exciting wavelength of a third harmonic of an Nd:YAG Q-switched laser (Brilliant B from Quantel) with a pulse duration of 4 ns and a repetition rate of 10 Hz was used, with an average energy of 4 mJ/pulse. The 460 nm exciting wavelength of a tunable optical parametric oscillator (OPO) pumped by 355 nm (3W) of a Q-switched Nd-YAG laser was also used, with an average energy of 4 mJ per pulse. In both case, the laser line was filtered out by a high-pass glass filter, i.e., LP 385 when exciting at 355 nm and LP 475 for laser excitation at 460 nm to avoid signal saturation of the CCD. The PL curve is obtained by rate between PL experimental curve and transmittance spectrum of glass filter. All the measurements were taken at room temperature.

3. Results and discussion

PL emission is associated directly with localized states existing in the band gap. Fig. 1 illustrates PL spectra recorded at room temperature of BCT20 powders heat treated at 400, 450, 500, 550, 575 and 600 °C at two different excitation wavelengths: the 460 (Fig. 1a) and the 355 nm (Fig. 1b) wavelength of an Nd:YAG laser system.

A set of emission bands is clearly recorded under the two excitation wavelengths and the position of the band peak of each annealing condition shifts to a higher wavelength as the excitation wavelength increases. These two distinct energies (3.52 and 2.72 eV) are able to excite different populations of electrons existing in the additional levels in the forbidden band gap of disordered samples. The BCT20 powder displays the most intense emission when excited at 355 nm.

The profile of the emission band is typical of a multiphonon and multilevel process, i.e., a system in which relaxation occurs by several paths, involving the participation of numerous states within the band gap of the material. This behavior is related to the structural disorder of BCT20 and confirms the presence of additional electronic levels in the forbidden band gap of the material [23].

The BCT20 powder annealed at 500 °C displays the most significant PL intensity when excited with these two laser beam wavelengths. Using the Gaussian method, the PL curves of the BCT20 sample annealed at 500 °C were decomposed into five components, each of which refers to the region in the visible spectrum where its maximum peak intensity appears. Each color represents a different type of electronic transition and can be linked to a specific structural arrangement. To gain a better understanding of the properties of PL and its dependence on the structural order–disorder of the lattice, the PL curves were analyzed using the PeakFit deconvolution program [24]. Based on the Gaussian line broadening mechanism for luminescence processes, the fine features in the PL spectra of samples annealed at 500 °C were deconvoluted and extracted from the deconvolution curves. Fig. 1c and d illustrates such decompositions, while Table 1 lists the areas under the curve of the respective transitions.

The decomposition band indicated the presence of different intermediate levels in the band gap. More energetic excitation wavelengths favor the transition of more energetic levels in the band gap. Thus, broadband PL emission consists of the sum of individual emissions. Such emissions arise from a radiative recombination between electrons and holes trapped in the gap states. The transitions of disordered titanates therefore occur at energies far below the band gap of these materials. The violet component is associated with more energetic transitions and is observed only after excitation with a laser beam wavelength of 355 nm. Otherwise, the green component is associated with a less energetic transition and is observed after excitation with a laser beam wavelength of 460 nm.

The PL property is affected by the relation between short- and long-range structural lattice order–disorder [15,16,20,23]. The relation between structural long-range order–disorder in BCT20 was determined using the XRD technique. Fig. 2 shows the XRD patterns of the BCT20 powders heat treated at different

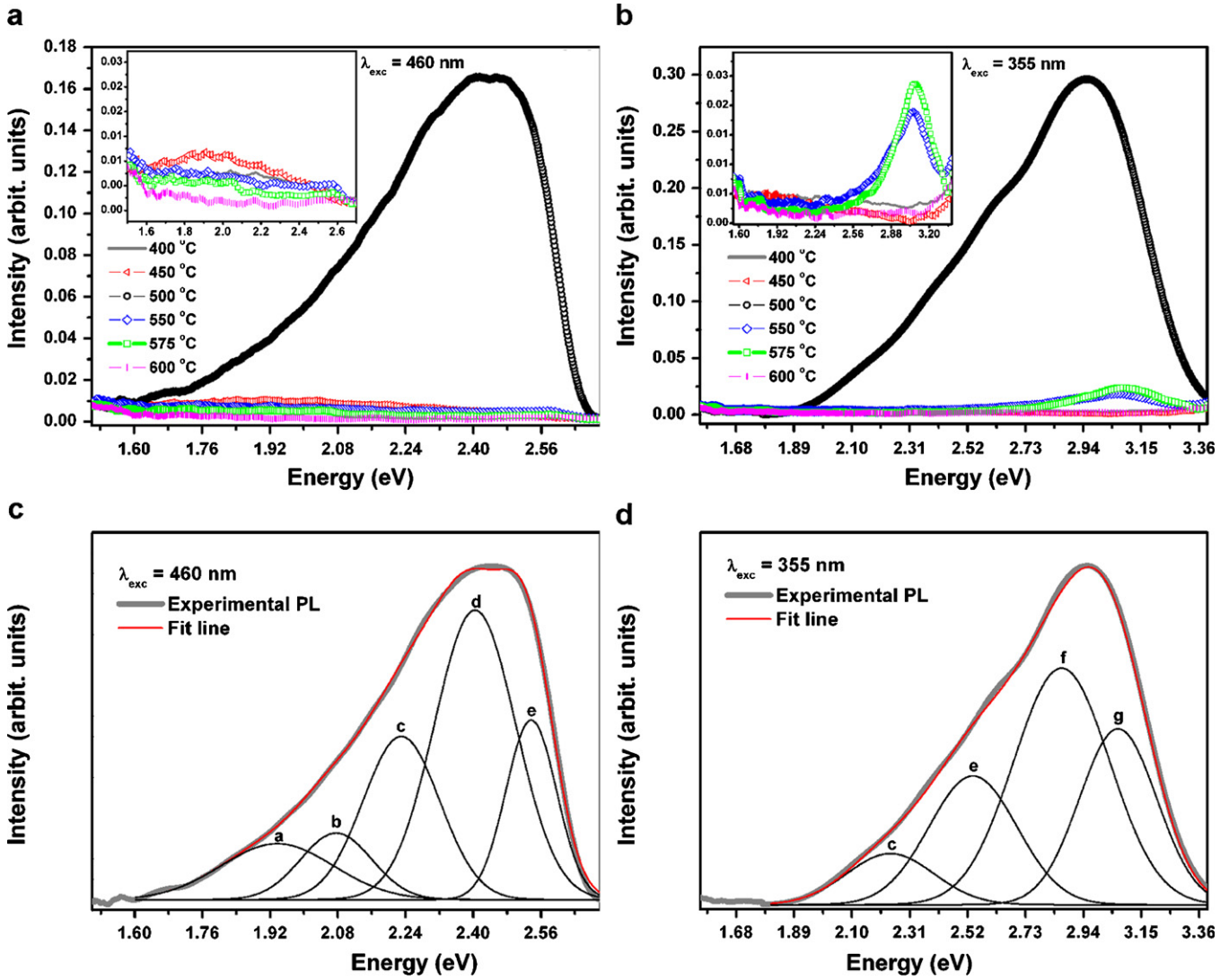

Fig. 1. Photoluminescence spectra at room temperature of BCT20 powder samples annealed at 400, 450, 500, 550, 575 and 600 °C with (a) excitation wavelength of 460 nm and (b) excitation wavelength of 355 nm. Deconvolution results of BCT20 heat treated at 500 °C: (c) excitation wavelength of 460 nm and (d) excitation wavelength of 355 nm.

Table 1
Fitting parameters of five Gaussian peaks.

BCT20 annealed at 500 °C							
Peak center (eV)							
λ (nm)	1.94 (a) RC	2.07 (b) YC	2.23 (c) GC	2.40 (d) GC	2.53 (e) BC	2.86 (f) VC	3.03 (g) VC
355 nm %[a]	0	0	8.6	0	21.8	43.6	26.0
460 nm %[a]	11.2	8.5	22.3	41.8	16.2	0	0

VC = violet component of PL; BC = blue component of PL; GC = green component of PL; YC = yellow component of PL; RC = red component of PL. Letters (a–g) correspond to components displayed in Fig. 1c and d.

[a] Percentage obtained by dividing the area of each decomposed PL curves by the total PL area.

temperatures ranging from 400 to 600 °C. All the diffraction peaks displayed by the BCT20 powder annealed at 600 °C were related to single-phase $BaTiO_3$ and this powder was completely indexed on the basis of the tetragonal structure presented in ICDD card no. 05-0626 (P4mm) [2,4,25–28]. No other peaks were observed, indicating a complete reaction to form the $(Ba_{0.8}Ca_{0.2})TiO_3$ [14,29,30].

Fig. 2 indicates that the BCT20 powders annealed at temperatures below 575 °C did not display diffraction peaks related to BCT20 phase. Diffraction peaks for BCT20 phase began to appear in the sample annealed at higher temperatures, and when the material was annealed at 600 °C it presented complete long-range structural order. This indicates that the samples annealed in the range of 400–550 °C did not show long-range order.

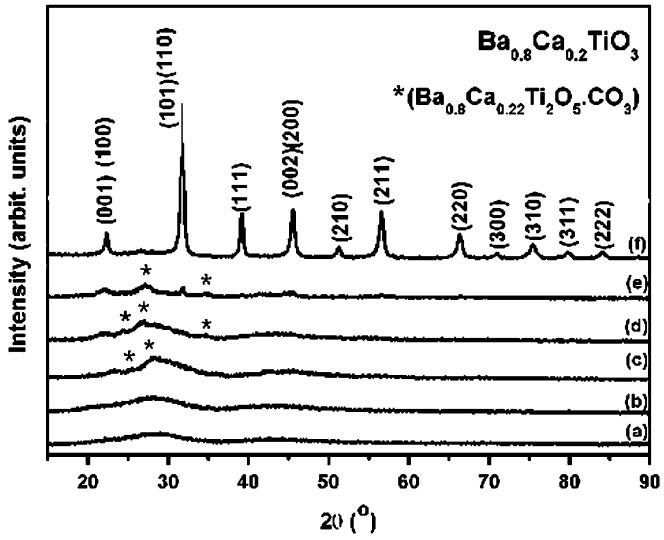

Fig. 2. XRD of BCT20 powders annealed at (a) 400, (b) 450, (c) 500, (d) 550, (e) 575 and (f) 600 °C.

The XRD analysis serves to explain PL results. The photoluminescence was due to BCT material and was not linked to the organic material remaining in the sample.

The literature contains numerous reports indicating that extending annealing times [31,32] and raising heat-treatment temperatures [33] reduce the amount of organic material in powders obtained by the PPM method. In fact, the BCT20 sample heat treated at 400 and 450 °C obviously contained more organic material and presented lower PL intensity than the BCT20 sample annealed at 500 °C.

The samples annealed at 500, 550 and 575 °C displayed diffractions peaks at 2θ~24.3°, 26.7° and 34.7° related to barium titanium oxycarbonate. Duran et al. [13] stated that this intermediate phase is already present in barium titanate powders heat treated at lower temperatures, e.g., at 430 °C. The intermediate oxycarbonate phase can be ruled out as being responsible for PL emission, since this phase was present in the BCT20 powders annealed at 550 and 575 °C, and these powders displayed very low PL intensity.

In addition to this structural long-range order study, the local structure was evaluated by XANES spectroscopy, considering the most representative samples. Fig. 3 shows the Ti K-edge XANES spectra of BCT20 samples as a function of the heat-treatment temperature.

The XANES spectra of powder samples annealed at 600 °C revealed that the local structure around titanium atoms was characteristic of the BCT20 crystalline compound with only hexacoordinated TiO_6 [34,35]. On the other hand, the XANES spectra of the samples annealed at 400, 500 and 550 °C showed a characteristic mixed local structure containing sixfold and fivefold titanium coordination, with TiO_5 units forming a pyramidal structure containing four oxygen atoms at the basal plane, and one at the apex [18]. The sixth oxygen atom belonging to the TiO_6 octahedron of the crystallized samples was located at a greater distance from the titanium atom. This sixth oxygen atom joins the other five oxygen atoms to form TiO_6 octahedron when the annealing temperature is increased [16,20]. The observation of a broad peak after the edge on these samples when compared with the crystalline ones could also be interpreted as representing a certain degree of disorder in the short- and medium-range environment around titanium atoms.

The Ca K-edge XANES results obtained by Lazaro et al. [18] in their study of the PL process in CT compounds pointed to the

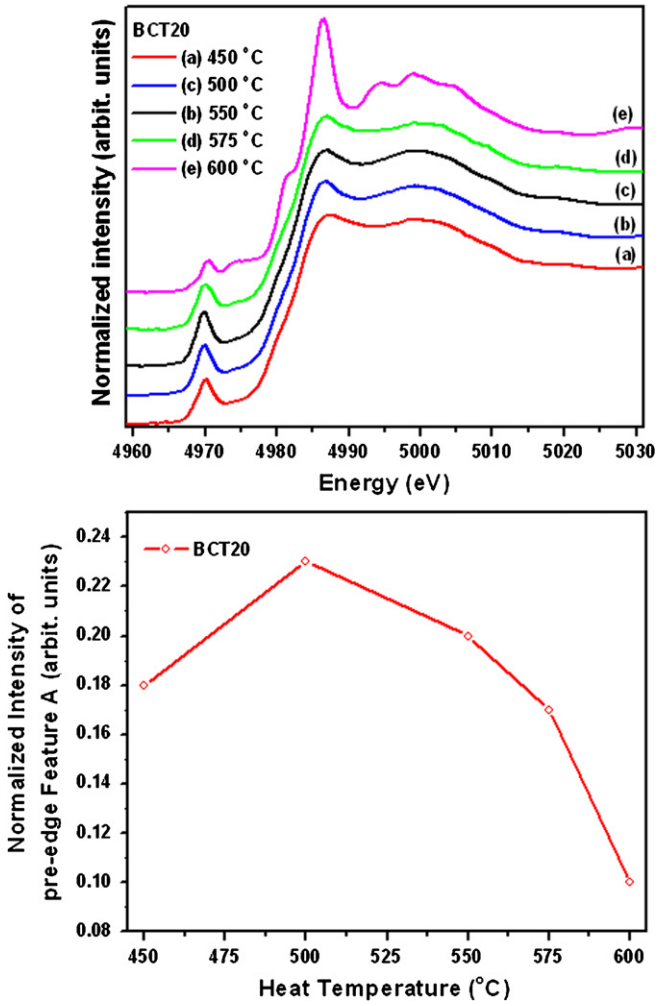

Fig. 3. (a) Ti K-edge XANES spectra of BCT20 powders annealed at 450, 500, 550, 575 and 600 °C; (b) normalized pre-edge A feature as a function of annealing temperature.

presence of different Ca coordination numbers, namely $Ca–O_{11}$ and $Ca–O_{12}$, in $CaTiO_3$. These authors showed that the modifier (Ca atom) and the former (Ti atom) lattice strongly affect the intensity of PL emission. It is therefore reasonable to assume that, in the BCT20 powders, the modification in the local environment around calcium and barium ions also led to significant changes in the electronic structure of the BCT20 samples.

The physical origin of the pre-edge feature A in Fig. 3 is the transition of the metallic 1s electron to an unfilled d state. This forbidden electronic transition dipole is normally allowed by the mixture of p states from surrounding oxygen atoms into the unfilled d states of titanium atoms [36].

The height and energy position of the pre-edge A feature can be attributed to the amount of TiO_6 and TiO_5 structural units present in the sample [36]. Fully structurally ordered BCT20 does not show PL emission, since all the Ti atoms are coordinated to six oxygen atoms in a completely regular octahedron. Hence, the sample containing 100% of TiO_6 served as a reference in the XANES experiments. In this work, the pre-edge A feature was fitted using a Gaussian function to determine its height and to relate this height to the TiO_5 concentration.

As indicated in Fig. 3b, the height of the pre-edge feature A peak varied as a function of the annealing temperature. An approximate TiO_5/TiO_6 ratio of 40/60 was found for samples

annealed in the 500–550 °C range. As expected, the amount of TiO_5 decreased as the annealing temperature increased.

The XRD and XANES results confirmed that short- and long-range structural order–disorder can be related directly to PL emission. At room temperature, the PL phenomenon occurs due to the structural disorder existing in the system. Therefore, if the system's structure is totally ordered (sample annealed at 600 °C), PL emission is absent.

4. Conclusions

The PL emission observed in the BCT20 powders after excitation with a laser beam wavelength of 355 and 460 nm may be associated with a certain degree of order–disorder in the structure of these samples. The BCT20 sample annealed at 500 °C presented high PL emission. The presence of intermediate oxycarbonate phase is not linked to PL emission. XANES experiments indicated the coexistence of two types of coordination for titanium, which is also associated with PL emission behavior. The amount of TiO_5 decreased as the temperature increased and PL emission decreased. This behavior was related to the structural disorder of BCT20 and confirmed the presence of additional electronic levels in the forbidden band gap of the material. These electronic levels allow for PL emission in BCT powder at room temperature.

Acknowledgments

The authors gratefully acknowledge the financial support of the Brazilian research financing Institutions FAPESP/CEPID, CNPq and CAPES. This research was partially performed at LNLS-National Laboratory of Synchrotron Light, Campinas, Brazil.

References

[1] M. Yashima, T. Hoshina, D. Ishimura, S. Kobayashi, W. Nakamura, T. Tsurumi, S. Wada, J. Appl. Phys. 98 (2005) 014313.
[2] P. Victor, R. Ranjith, S.B. Krupanidhi, J. Appl. Phys. 94 (2003) 7702.
[3] J.C. Chen, C.Y. Chen, J. Cryst. Growth 236 (2002) 640.
[4] C. Kuper, R. Pankrath, H. Hesse, Appl. Phys. A-Mater. Sci. Process. 65 (1997) 301.
[5] G. Roosen, S. Bernhardt, P. Delaye, Opt. Mater. 23 (2003) 243.
[6] S. Bernhardt, H. Veenhuis, P. Delaye, G. Roosen, Opt. Mater. 18 (2001) 13.
[7] H. Veenhuis, T. Borger, K. Peithmann, M. Flaspohler, K. Buse, R. Pankrath, H. Hesse, E. Kratzig, Appl. Phys. B-Lasers Opt. 70 (2000) 797.
[8] H. Veenhuis, T. Borger, K. Buse, C. Kuper, H. Hesse, E. Kratzig, J. Appl. Phys. 88 (2000) 1042.
[9] N. Korneev, D. Mayorga, S. Stepanov, H. Veenhuis, K. Buse, C. Kuper, H. Hesse, E. Kratzig, Opt. Commun. 160 (1999) 98.
[10] N. Korneev, D. Mayorga, H. Veenhuis, K. Buse, E. Kratzig, J. Opt. Soc. Am. B-Opt. Phys. 16 (1999) 1725.
[11] N. Korneev, H. Veenhuis, K. Buse, E. Kratzig, J. Opt. Soc. Am. B-Opt. Phys. 18 (2001) 1570.
[12] L. Jastrabik, S.E. Kapphan, V.A. Trepakov, I.B. Kudyk, R. Pankrath, J. Lumin. 102 (2003) 657.
[13] P. Duran, D. Gutierrez, J. Tartaj, M.A. Banares, C. Moure, J. Eur. Ceram. Soc. 22 (2002) 797.
[14] S. Kumar, G.L. Messing, W.B. White, J. Am. Ceram. Soc. 76 (1993) 617.
[15] P.S. Pizani, H.C. Basso, F. Lanciotti, T.M. Boschi, F.M. Pontes, E. Longo, E.R. Leite, Appl. Phys. Lett. 81 (2002) 253.
[16] M.F.C. Gurgel, J.W.M. Espinosa, A.B. Campos, I.L.V. Rosa, M.R. Joya, A.G. Souza, M.A. Zaghete, P.S. Pizani, E.R. Leite, J.A. Varela, E. Longo, J. Lumin. 126 (2007) 771.
[17] V.M. Longo, L.S. Cavalcante, A.T. de Figueiredo, L.P.S. Santos, E. Longo, J.A. Varela, J.R. Sambrano, C.A. Paskocimas, F.S. De Vicente, A.C. Hernandes, Appl. Phys. Lett. 90 (2007) 091906.
[18] S. de Lazaro, J. Milanez, A.T. de Figueiredo, V.M. Longo, V.R. Mastelaro, F.S. De Vicente, A.C. Hernandes, J.A. Varela, E. Longo, Appl. Phys. Lett. 90 (2007) 111904.
[19] A.T. de Figueiredo, V.M. Longo, S. de Lazaro, V.R. Mastelaro, F.S. De Vicente, A.C. Hernandes, M. Siu Li, J.A. Varela, E. Longo, J. Lumin. 126 (2007) 403.
[20] E. Longo, E. Orhan, F.M. Pontes, C.D. Pinheiro, E.R. Leite, J.A. Varela, P.S. Pizani, T.M. Boschi, F. Lanciotti, A. Beltran, J. Andres, Phys. Rev. B 69 (2004) 125115.
[21] F.V. Motta, A.P.A. Marques, M.T. Escote, D.M.A. Melo, A.G. Ferreira, E. Longo, E.R. Leite, J.A. Varela, J. Alloys Compd. 465 (2008) 452.
[22] A.P.A. Marques, D.M.A. de Melo, C.A. Paskocimas, P.S. Pizani, M.R. Joya, E.R. Leite, E. Longo, J. Solid State Chem. 179 (2006) 671.
[23] A.T. de Figueiredo, S. de Lazaro, E. Longo, E.C. Paris, J.A. Varela, M.R. Joya, P.S. Pizani, Chem. Mater. 18 (2006) 2904.
[24] T. Ding, W.T. Zheng, H.W. Tian, J.F. Zang, Z.D. Zhao, S.S. Yu, X.T. Li, F.L. Meng, Y.M. Wang, X.G. Kong, Solid State Commun. 132 (2004) 815.
[25] V.S. Tiwari, D. Pandey, P. Groves, J. Phys. D-Appl. Phys. 22 (1989) 837.
[26] W.S. Cho, J. Phys. Chem. Solids 59 (1998) 659.
[27] Y.I. Kim, J.K. Jung, K.S. Ryu, Mater. Res. Bull. 39 (2004) 1045.
[28] J.D. Tsay, T.T. Fang, T.A. Gubiotti, J.Y. Ying, J. Mater. Sci. 33 (1998) 3721.
[29] T. Mazon, A.C. Hernandes, A.G. Souza, A.P.A. Moraes, A.P. Ayala, P.T.C. Freire, J. Mendes, J. Appl. Phys. 97 (2005) 104113.
[30] V.S. Tiwari, D. Pandey, J. Am. Ceram. Soc. 77 (1994) 1819.
[31] F.M. Pontes, C.D. Pinheiro, E. Longo, E.R. Leite, S.R. de Lazaro, J.A. Varela, P.S. Pizani, T.M. Boschi, F. Lanciotti, Mater. Chem. Phys. 78 (2003) 227.
[32] P.S. Pizani, E.R. Leite, F.M. Pontes, E.C. Paris, J.H. Rangel, E.J.H. Lee, E. Longo, P. Delega, J.A. Varela, Appl. Phys. Lett. 77 (2000) 253.
[33] A.P.A. Marques, F.C. Picon, D.M.A. Melo, P.S. Pizani, E.R. Leite, J.A. Varela, E. Longo, J. Fluoresc. 18 (2008) 51.
[34] K. Asokan, J.C. Jan, J.W. Chiou, W.F. Pong, M.H. Tsai, H.L. Shih, H.Y. Chen, H.C. Hsueh, C.C. Chuang, Y.K. Chang, Y.Y. Chen, I.N. Lin, J. Phys. -Condes. Matter 13 (2001) 11087.
[35] K. Asokan, J.C. Jan, J.W. Chiou, W.F. Pong, M.H. Tsai, Y.K. Chang, Y.Y. Chen, H.H. Hsieh, H.J. Lin, Y.W. Yang, L.J. Lai, I.N. Lin, J. Solid State Chem. 177 (2004) 2639.
[36] F. Farges, G.E. Brown, J.J. Rehr, Phys. Rev. B 56 (1997) 1809.